Domino model for geomagnetic field reversals

N. Mori,[1] D. Schmitt,[2,*] J. Wicht,[2] A. Ferriz-Mas,[3,4] H. Mouri,[5] A. Nakamichi,[6] and M. Morikawa[1]
[1]*Department of Physics, Ochanomizu University, Tokyo 112-8610, Japan*
[2]*Max-Planck-Institut für Sonnensystemforschung, 37191 Katlenburg-Lindau, Germany*
[3]*Departamento de Física Aplicada, Universidad de Vigo, 32004 Orense, Spain*
[4]*Instituto de Astrofísica de Andalucía, IAA-CSIC, 18080 Granada, Spain*
[5]*Meteorological Research Institute, Tsukuba 305-0052, Japan*
[6]*Koyama Astronomical Observatory, Kyoto Sangyo University, Kyoto 603-8555, Japan*
(Received 24 October 2011; revised manuscript received 5 September 2012; published 9 January 2013)

We solve the equations of motion of a one-dimensional planar Heisenberg (or Vaks-Larkin) model consisting of a system of interacting macrospins aligned along a ring. Each spin has unit length and is described by its angle with respect to the rotational axis. The orientation of the spins can vary in time due to spin-spin interaction and random forcing. We statistically describe the behavior of the sum of all spins for different parameters. The term "domino model" in the title refers to the interaction among the spins. We compare the model results with geomagnetic field reversals and dynamo simulations and find strikingly similar behavior. The aggregate of all spins keeps the same direction for a long time and, once in a while, begins flipping to change the orientation by almost 180 degrees (mimicking a geomagnetic reversal) or to move back to the original direction (mimicking an excursion). Most of the time the spins are aligned or antialigned and deviate only slightly with respect to the rotational axis (mimicking the secular variation of the geomagnetic pole with respect to the geographic pole). Reversals are fast compared to the times in between and they occur at random times, both in the model and in the case of the Earth's magnetic field.

DOI: 10.1103/PhysRevE.87.012108 PACS number(s): 05.50.+q, 47.27.eb, 75.10.Hk, 91.25.−r

I. INTRODUCTION

One of the most remarkable phenomena of geomagnetism is that the Earth has reversed the polarity of its almost dipolar magnetic field many times in the past at irregular intervals [e.g., [1,2]. Similar reversals have also been observed in turbulent dynamo experiments [3] and in simulations of the geodynamo [4], but the cause of the reversals has eluded a convincing explanation [5].

The magnetic field of the Earth originates from dynamo action in the liquid outer core [e.g., [6]. Helical flows in convection columns that encircle the inner core tangent cylinder and are aligned with the rotation axis play an important role for the magnetic field generation [7,8]. Numerical simulations of the geodynamo successfully reproduce many features of the magnetic field of the Earth, including stochastic reversals [e.g., [9]. Depending on the importance of the inertial forces relative to the rotational forces, dynamos with either a dominant axial dipole or with a small-scale multipolar magnetic field are found [10]. The transition from dipolar to multipolar dynamos takes place at a local Rossby number of approximately 0.1 [11]. The Earth lies close to the transition between both types [12], which may explain why the dipole undergoes sporadic reversals.

In weakly driven dynamos, the helical convection columns generate an axial dipole, while in strongly driven dynamos, the flow and the field have smaller spatial structures and chaotically fluctuate in time. Direct numerical simulations of the geodynamo are computationally expensive and thus only a few reversals have been studied in detail. Typically these simulations show that reversals go along with a breaking of the north-south (equatorial) symmetry in the flow of the aligned fluid columns. Sporadic flow upwellings, when transporting inverse magnetic flux patterns from the inner core to the core mantle boundaries, seem to trigger polarity reversals [13]. To some extent, the upwellings behave like tilted convective columns, at least where their role in the dynamo mechanism is concerned. We will further discuss this issue in Sec. V.

The reversal sequences in paleomagnetic data and in dynamo models have been analyzed for their statistical properties. First estimates that geomagnetic reversals obey a Poissonian process where all reversals are independent of each other do not describe all statistical features of the reversal record. The statistical reversal rate has likely been changing over time due to the varying heat flux through the core-mantle boundary [14–17]. The reversal sequence also suggests that the process may have a short- and a long-term memory, leading to changes in the statistical behavior and the characterizing distribution function of the times between reversals [18,19]. Similar analysis for fully 3D numerical dynamo simulations are rare because it is very costly to compile a large number of reversals. The analysis by Wicht *et al.* [20] and Driscoll and Olson [16] indicate that the numerical simulations may follow similar reversal statistics as the paleomagnetic record.

Simple parameterized models allow for a large number of reversals, so that a statistical analysis becomes more meaningful. A famous example is the two-disk dynamo of Rikitake [21], which exhibits sporadic reversals, but also a cyclic variation of the dipole moment during stable polarity periods. The extensions to N-coupled disks by Shimizu and Honkura [22] and Ito [23] improved on the latter weak point. Hoyng *et al.* [24] considered a mean-field dynamo model with stochastic fluctuations of the induction effect; these lead to oscillations of the dipole field amplitude in a bistable potential with minima representing normal and reversed polarity and occasional jumps between them [25].

*schmitt@mps.mpg.de

Here we study another class of simplified models, an Ising-Heisenberg model of interacting magnetic spins. Ising-like models have been used in molecular dynamics and statistical mechanics for describing, for instance, phase transitions in ferromagnetism, for modeling spin glasses, and for pattern recognition in neural networks [e.g., [26]]. Coupled spin models of Ising type, where the individual spins can assume two scalar states $+1$ or -1 and interact with each other after certain rules, have also been suggested for describing geomagnetic polarity reversals and their statistics [27–29]. We analyze a planar Heisenberg model consisting of a system of vectorial spins aligned along a ring. Each spin has unit length and is described by its angle with respect to the rotational axis, i.e., each spin has one degree of freedom. The orientation of the spins can vary in time due to spin-spin interaction and random forcing. The consecutive interaction of adjacent spins is described as "domino model." We consider the time dependence of the average orientation of all spins, which exhibits a similar behavior as the geomagnetic reversal record.

These sorts of models are often classified according to spatial dimensionality and number of components of spin vectors. Our model is one-dimensional (i.e., spatial dimensionality of the lattice is one) and vectors (spins) are two-dimensional (i.e., they are contained within a plane). Thus, the domino model is a one-dimensional XY model, also referred to as the plane rotator model or the Vaks-Larkin model [30]. Spin vectors in Ising and Heisenberg models are 1D and 3D, respectively. A clear classification can be found in the classic textbook by Stanley [31].

The spins in our model might be associated with the convection columns, whose electromagnetic induction generates elementary dipoles. The tendency of the spins to be aligned with the rotation axis is a consequence of the Proudman-Taylor theorem, and the time variation of the spins is a measure of the vigor of convection and of the sporadic upwellings. The convective columns represent building blocks of the full dynamo process. Their interaction is modeled here by the spins in the simple domino model. It turns out that this model successfully describes the statistics of geomagnetic reversals, which indicates that the polarity reversals may be understood by the collective interaction of these columns. The model does not, however, describe the details of the dynamo process in the individual convection columns.

The structure of the paper is as follows. In Sec. II, the model is described. The results and the statistical analysis of our model are presented in Sec. III. The influence of the various parameters as well as alternative model descriptions are given in Sec. IV. The results are compared with numerical dynamo simulations in Sec. V and with geomagnetic data in Sec. VI. In Sec. VII, we give our conclusions.

II. THE DOMINO MODEL

A. Model equations

We consider a system of N macrospins aligned along a ring and interacting pairwise like in a one-dimensional Vaks-Larkin model. The spins are embedded in a uniformly rotating medium and we take $\mathbf{\Omega} = (0,1)$ as the unit vector along the rotational axis. Each spin $\boldsymbol{S}_i$, $i = 1,\ldots,N$ has unit length and is described by its angle θ_i with respect to the rotational axis, such that $\boldsymbol{S}_i = (\sin\theta_i, \cos\theta_i)$. The orientation of the spins can vary in time due to random forcing and spin-spin interaction (Fig. 1).

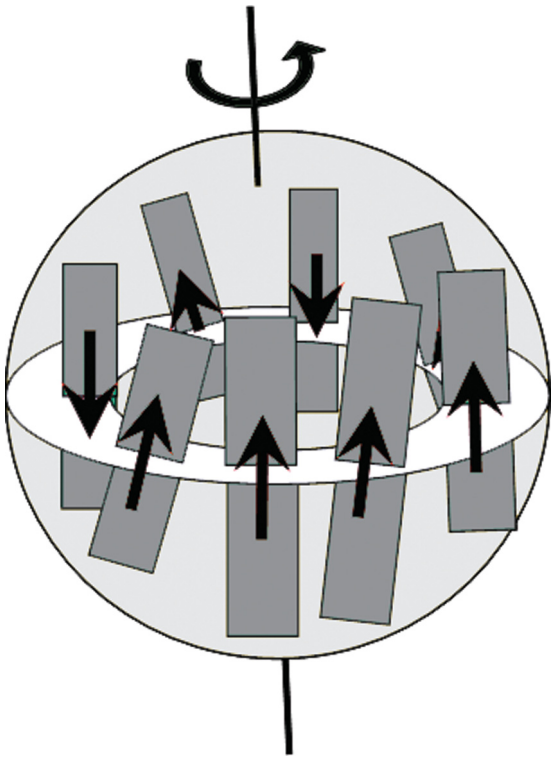

FIG. 1. (Color online) Sketch of the domino model.

The kinetic and the potential energy $K(t)$ and $P(t)$ of the system are

$$K(t) = \frac{1}{2}\sum_{i=1}^{N}\dot{\theta}_i(t)^2\,, \tag{1}$$

$$P(t) = \gamma\sum_{i=1}^{N}(\mathbf{\Omega}\cdot\boldsymbol{S}_i)^2 + \lambda\sum_{i=1}^{N}(\boldsymbol{S}_i\cdot\boldsymbol{S}_{i+1}), \tag{2}$$

where $i+1 = 1$ when $i = N$. Here, γ is a parameter characterizing the tendency of the spins to be aligned with the rotation axis, while λ is a parameter characterizing the spin-spin interaction. The scalar product to the square in the γ-term ensures that there is no preferred polarity. The interaction is such that each spin interacts with the two neighboring spins: spin 2 interacts with spins 1 and 3, spin 3 with spins 2 and 4, and so on. Spin N interacts with spins $N-1$ and 1; i.e., we are considering periodic boundary conditions and, therefore, talk about a ring system here.

The Lagrangian for the system is $\mathcal{L} = K - P$. We set up a Langevin-type equation as follows:

$$\frac{\partial}{\partial t}\left(\frac{\partial\mathcal{L}}{\partial\dot{\theta}_i}\right) = \frac{\partial\mathcal{L}}{\partial\theta_i} - \kappa\dot{\theta}_i(t) + \frac{\epsilon\chi_i}{\sqrt{\tau}}, \tag{3}$$

where the term $-\kappa\dot{\theta}_i(t)$ describes friction and the term $\epsilon\chi_i/\sqrt{\tau}$ is a random force acting on each spin. The parameters κ and ϵ characterize the strengths of the friction and the random forcing, respectively. Finally, χ_i is a Gaussian-distributed

random number with zero mean and unit variance associated to each spin, which is updated each correlation time τ.

Inserting the expressions for the kinetic and potential energy, Eqs. (1) and (2), into Eq. (3) yields

$$\ddot{\theta}_i - 2\gamma \cos\theta_i \sin\theta_i + \lambda[\cos\theta_i(\sin\theta_{i-1} + \sin\theta_{i+1}) - \sin\theta_i(\cos\theta_{i-1} + \cos\theta_{i+1})] + \kappa\dot{\theta}_i - \frac{\epsilon\chi_i}{\sqrt{\tau}} = 0, \quad i = 1,\ldots,N, \tag{4}$$

with $\theta_0 = \theta_N$ and $\theta_{N+1} = \theta_1$.

We integrate the equations of motion [Eq. (4)] forward in time with a fourth-order Runge-Kutta scheme starting from a random orientation of the spins between 0 and 2π. A standard set of parameters N, γ, λ, κ, ϵ, and τ is considered in Sec. III, while the parameter dependence of the mean time between reversals is studied in Sec. IV A. In Sec. IV B, we also slightly alter the model using different alternatives of the γ term, the λ term, and the forcing term.

As main output we consider the cumulative orientation of all spins and define

$$M(t) = \frac{1}{N}\sum_{i=1}^{N} \boldsymbol{\Omega}\cdot\boldsymbol{S}_i(t) = \frac{1}{N}\sum_{i=1}^{N}\cos\theta_i(t) \tag{5}$$

as the resulting total axial magnetic moment or "magnetization."

B. Assessment of numerical stability

We tested that the results are insensitive to the employed numerical method. For the Runge-Kutta scheme, for instance, we reduced the integration time step Δt by factors of 2, 5, and 10 compared to the model of Sec. III without qualitative and quantitative change of the results.

We furthermore implemented two different algorithms from the ODEPACK [32], a predictor-corrector scheme after Adams (suitable for nonstiff systems) and a backward differentiation scheme after Gear (for stiff cases). In both cases, the step-size was adaptive and controlled by relative and absolute error tolerances. Both gave the same results as the Runge-Kutta scheme once the error tolerances were chosen small enough, e.g., relative error bounds equal zero and absolute error bounds equal 10^{-10} for θ_i.

Although the particular times at which reversals occurred varied, the overall statistical behavior did not change when we reduced the time step of the Runge-Kutta routine or when we employed the other integration algorithms. Both the mean time and the distribution of times between reversals as well as the power spectrum and the distribution of the magnetization were all the same within the statistical margins.

We conclude from this that the results of the domino model are numerically robust and we can stay with the computationally less expensive Runge-Kutta method.

III. RESULTS AND STATISTICAL ANALYSIS OF A TYPICAL MODEL

The parameters of our standard model are $N = 8$, $\gamma = -1$, $\lambda = -2$, $\kappa = 0.1$, $\epsilon = 0.4$, and $\tau = 0.01$. The integration time step was $\Delta t = 0.01$, the total number of time steps was 3×10^7, and every 10th time step is outputted. The run comprises a total of 824 reversals, i.e., the mean time between reversals is 364. Identifying this time with the mean time between reversals in the case of the Earth, which is 300 kyr, the whole run with a time of 300 000 spans approximately 250 Myr. The length of the run is not limited by numerical constraints, but the number of 824 reversals is large enough for a robust statistical comparison with the available geomagnetic record of 332 reversals (see Sec. VI). In Fig. 2 the first tenth of the full run is displayed.

The statistical analysis is based on the whole time series. The power spectrum is shown in Fig. 3(a). Over a large range comprising most of the reversals, the spectrum follows a power law with an exponent of about -1.7. The spectrum for small frequencies or long polarity chrons (i.e., epochs of one polarity) is flatter, while the steeper decrease at high frequencies comes from the fast variations between reversals. The distribution of the magnetization peaks near ± 1 with a wide and deep valley between them [Fig. 3(b)]. This reflects the fact that the flipping or reversal times are short events compared to the average duration time between them and that the spins are, most of the time, closely aligned with the rotation axis.

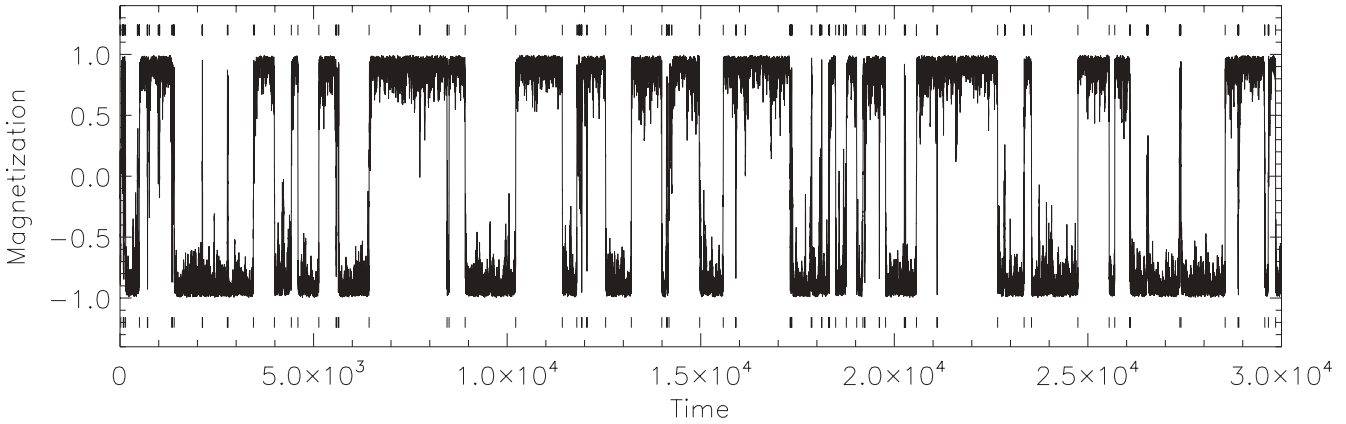

FIG. 2. The magnetization of the standard run as a function of time. At the top, the times of all zero-crossings are indicated (all reversals), while at the bottom, only those where a central band of $M = [-0.5, 0.5]$ is crossed are displayed (true reversals).

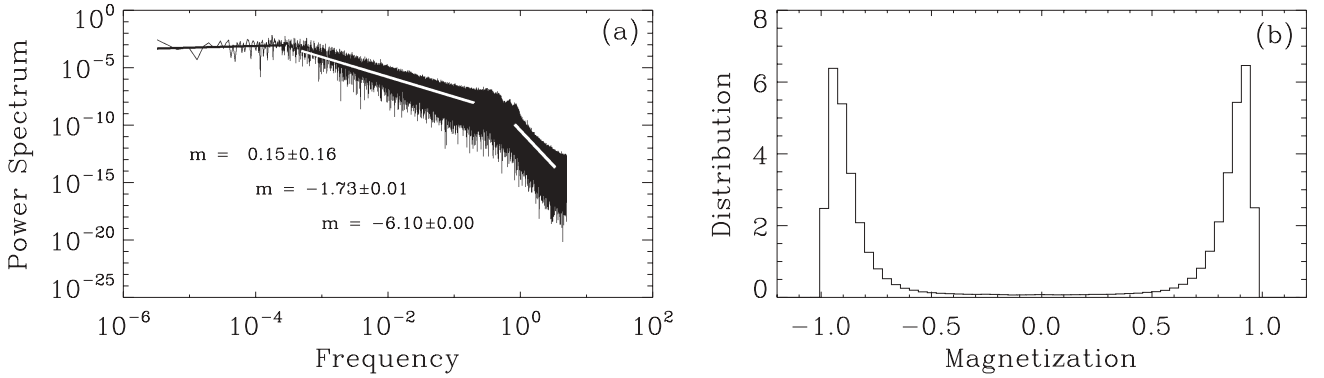

FIG. 3. (a) Log-log plot of the power spectrum of the magnetization. (b) Normalized distribution of the magnetization.

The distribution of the duration of long chrons follows a power law with an exponent of approximately −1.5 [Fig. 4(a)], while the short chrons are approximately exponentially distributed [Fig. 4(b)].

In Fig. 5, the details of one single reversal at $t \approx 3450$ are shown. The reversal is triggered by a large fluctuation of spin 4, which is successively transferred to the neighboring spins, which fluctuate until finally all spins reverse their polarity. We call our model "domino model" because of this consecutive interaction of neighboring spins. The duration of the full reversal depends on how fast the original fluctuation is transferred to all other spins. The reversal here lasts about 10 time units, which corresponds to 8 000 yr, roughly the time it takes for the geomagnetic field to flip polarity. Shortly afterwards, at $t \approx 3\,470$, some spins again show large variations and even reverse for a short time. Since they fail to transfer this to all the other spins, the total magnetization shows an excursion rather than a reversal. Examples of a true reversal, an aborted reversal, and two excursions are shown in Fig. 6.

IV. PARAMETER STUDY

The model contains a number of free parameters. The main quantity that depends sensitively on their values is the frequency of reversals. The statistical results, described in Sec. IV A, are based on many runs with at least three hundred reversals. When the time between reversals was longer than in our standard model of Sec. III we also had to execute these runs longer to achieve stable statistical results. The slope of the power spectrum depends only weakly on the model parameters. The distribution of the magnetization is also similar to the model of Sec. III. When there are very many reversals, the valley between the two stable states is less wide and deep.

A. Mean time between reversals

The dependence of the mean time between reversals on the number of spins is shown in Fig. 7. In the case of a few spins, this time steeply increases with the number, but it seems to saturate for a larger number of spins.

The parameter γ measures the tendency of the spins to be aligned with the rotation axis. Large negative values stabilize the orientation and lead to fewer reversals [Fig. 8(a)]. A value of $\gamma = 0$ still behaves like a bistable oscillator, but with many reversals and an almost flooded valley between the stable states in the distribution function. Positive values of γ do not lead to a stable magnetization but to oscillations around $M = 0$.

The influence of the spin-spin interaction parameter λ is similar. Large negative values stabilize [Fig. 8(b)]. For $\lambda \geqslant 0$ the system randomly oscillates around $M = 0$.

Increased friction, described by larger values of κ, quite naturally stabilizes [Fig. 8(c)], while increased random forcing, described by larger values of ϵ, destabilizes the

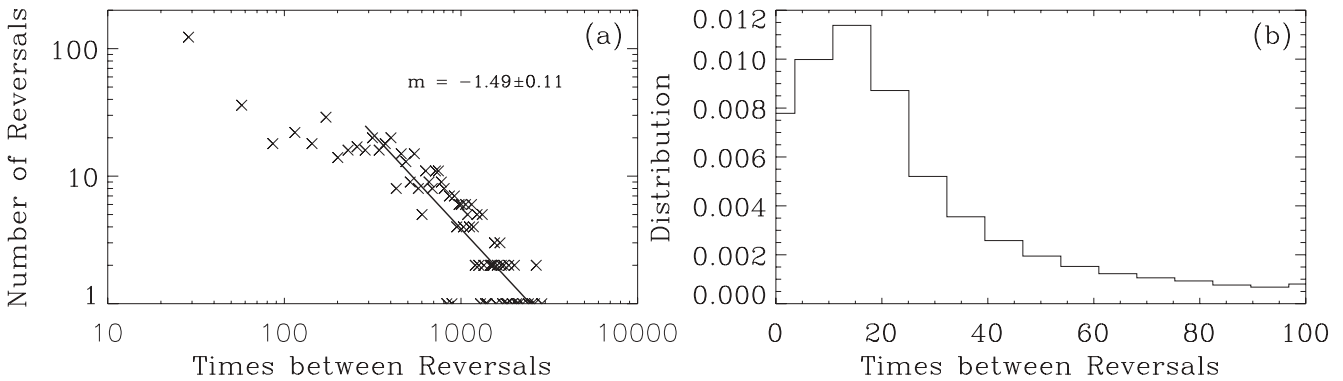

FIG. 4. (a) Log-log plot of the number of reversals as a function of the times between reversals. (b) Normalized distribution of the times between reversals for short duration chrons.

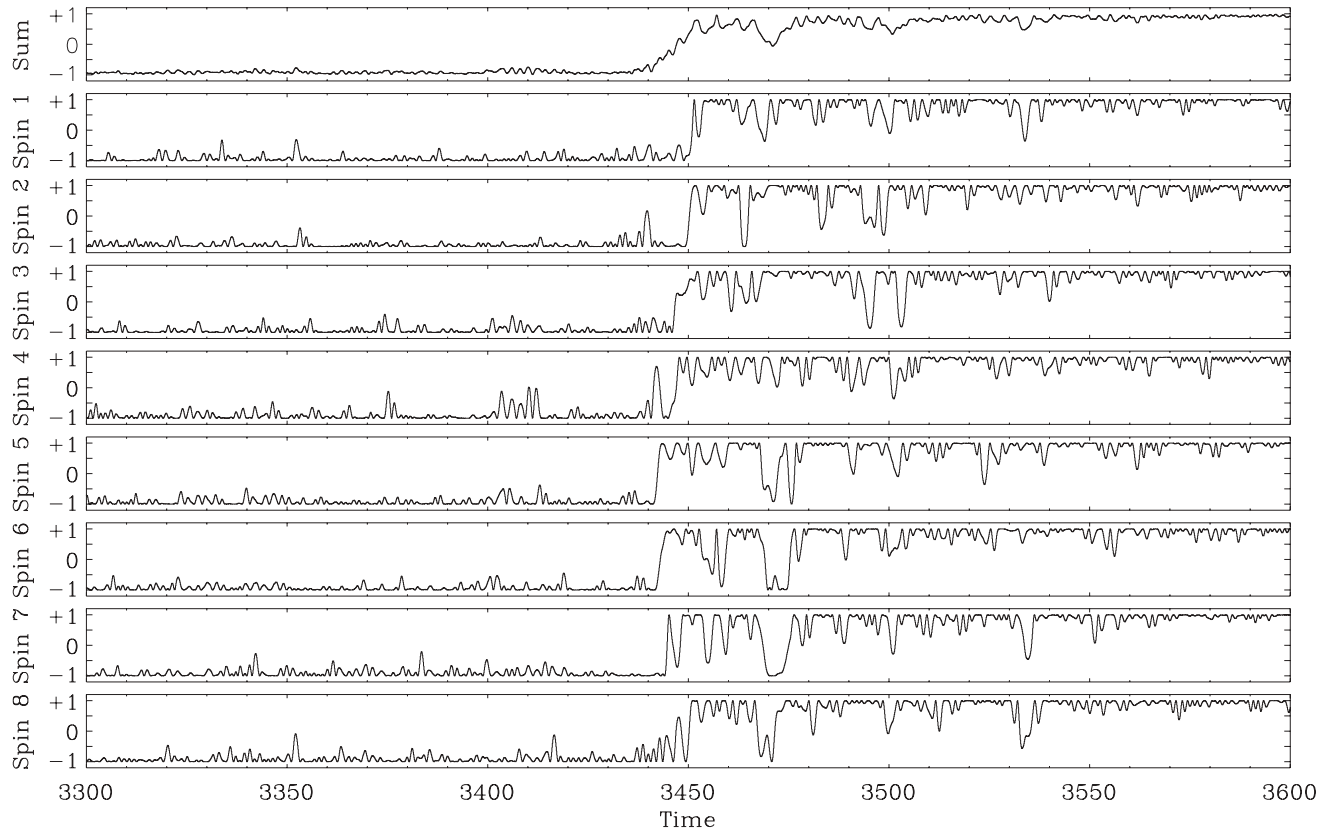

FIG. 5. The total magnetization of all spins, $\sum_{i=1}^{N} \cos\theta_i / N$ (top panel), and the magnetization of the individual spins, $\cos\theta_i$, before and after a reversal at $t \approx 3450$.

system, leading to shorter chrons and more frequent reversals [Fig. 8(d)].

The mean time between reversals depends sensitively on the model parameters. Thus, the drastic changes in the reversal frequency of the geomagnetic field could be explained by a moderate change of the model parameters with time.

B. Alternative model descriptions

We also tested to which degree the results depend on the details of the model setup. Instead of a γ term in Eq. (2) proportional to $\sum(\boldsymbol{\Omega} \cdot \boldsymbol{S}_i)^2$, we have considered a term proportional to $\sum |\boldsymbol{\Omega} \cdot \boldsymbol{S}_i|$. Since all $|\boldsymbol{\Omega} \cdot \boldsymbol{S}_i| \leqslant 1$ and, thus, $\sum |\boldsymbol{\Omega} \cdot \boldsymbol{S}_i| \geqslant \sum(\boldsymbol{\Omega} \cdot \boldsymbol{S}_i)^2$, very similar results were obtained

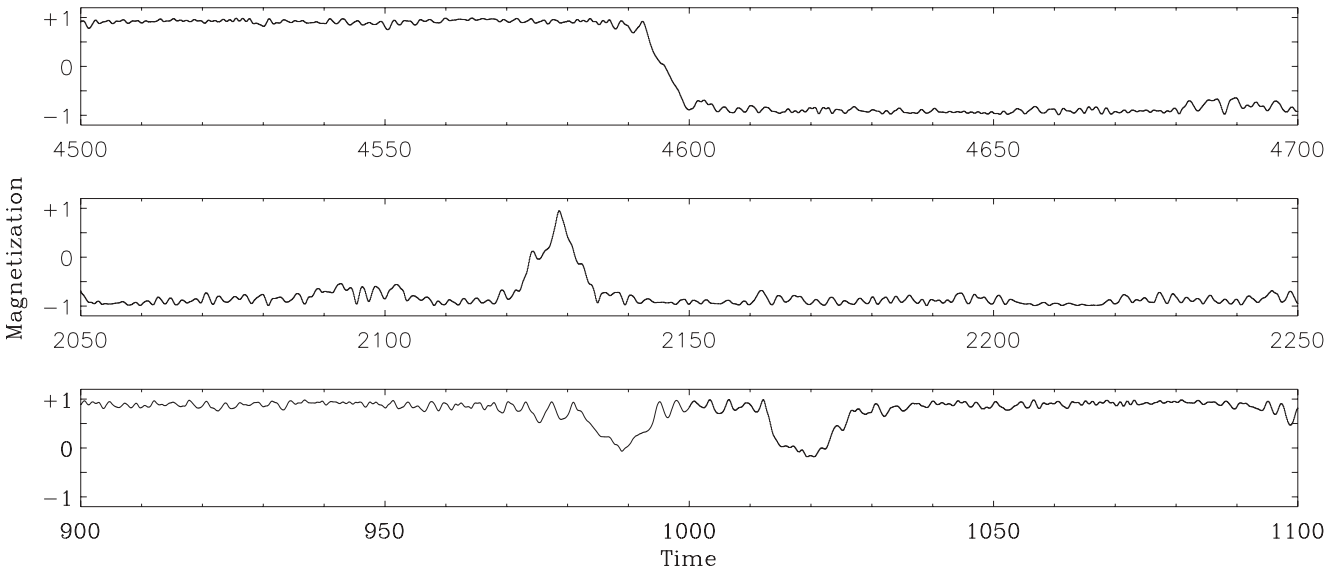

FIG. 6. Examples of a true reversal (top panel), an aborted reversal (middle panel), and two excursions (bottom panel).

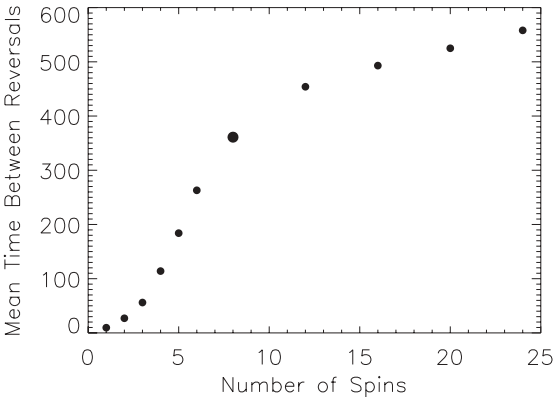

FIG. 7. The mean time between reversals depending on the number of spins N. The symbol for the standard model of Sec. III is plotted larger. The values of all other parameters are as in our standard model.

for somewhat smaller (absolute) values of γ. For a γ term proportional to $\sum(\boldsymbol{\Omega} \cdot \boldsymbol{S}_i)$, no reversals were observed.

Furthermore, instead of an additive forcing with Gaussian noise, described by the last term in Eq. (3), we also investigated white noise, which only results in somewhat less frequent reversals. Using multiplicative forcing proportional to $\cos\theta_i$ leads to much fewer reversals. Multiplicative forcing proportional to $\mathrm{mod}(\theta_i, 2\pi)$ yields random oscillations about 0 and, thus, not a very Earth-like reversal behavior.

As an alternative to the local interaction with neighboring spins only, described by the λ term in Eq. (2), we also considered a global or "mean-field" interaction with all other spins, described by $(2\lambda/N)\sum_{i<j}^{N}(\boldsymbol{S}_i \cdot \boldsymbol{S}_j)$. A normalization factor of $2/N$ is included in order to compare with the standard interaction with just the adjacent neighbors. The mean-field model results in less frequent reversals, but shows otherwise qualitatively similar behavior.

It is interesting to note that in globally coupled models a qualitatively similar behavior to the domino model described above is also found even without noise and without friction. The resulting system is conservative and only two parameters, γ and λ, are left. We study this system in detail in another paper [33].

V. COMPARISON WITH NUMERICAL DYNAMO SIMULATIONS

A direct comparison with numerical dynamo simulations is difficult. In our simplified spin model the dynamic equations only concern the relative angles of the spins to the rotation axis while a typical numerical dynamo deals with magnetic field, velocity, pressure, and temperature. Based on the close analysis of numerical simulations [4,5,13,17,20,34–40], see Fig. 9 as an example, we may nevertheless build some analogies, in particular concerning the reversal behavior.

Convection in fast rotating bodies like planetary liquid interiors organizes itself in the form of convective columns. They encircle the inner core tangent cylinder and are aligned in the z direction parallel to the rotation axis. The flow becomes quasi-two-dimensional (geostrophic), minimizing any variation in z direction according to the Taylor-Proudman

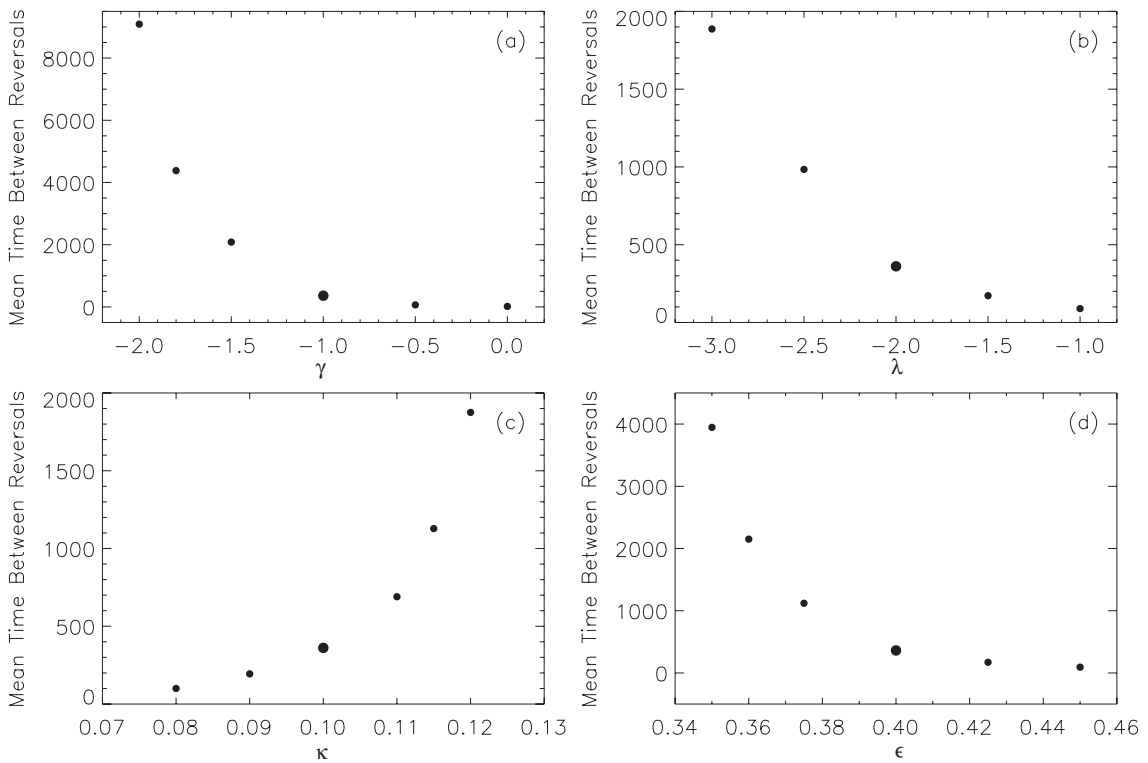

FIG. 8. The mean time between reversals depending on (a) γ, (b) λ, (c) κ, and (d) ϵ. The symbol for the standard model of Sec. III is plotted larger. All other parameters are as in our standard model.

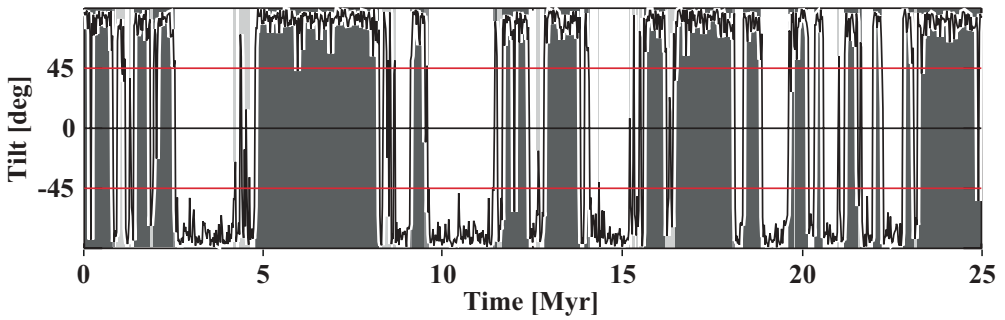

FIG. 9. (Color online) Dipole tilt angle in a MHD dynamo simulation with Ekman number $E = 2 \cdot 10^{-2}$, Rayleigh number Ra = 300, Prandtl number $P = 1$, and magnetic Prandtl number Pm = 10 (adapted from Ref. [20]).

theorem. Cyclonic and anticyclonic columns, rotating faster or slower than the planet, respectively, alternate in azimuthal direction [7]. In strongly driven dynamos, the number of columns increases. In addition to this primary rotation, there is a secondary flow along the axis of the individual columns, toward the equator in cyclonic and away from the equator in anticyclonic columns. Primary and secondary components taken together determine the helicity $\boldsymbol{U} \cdot (\nabla \times \boldsymbol{U})$, where $\boldsymbol{U}$ is the velocity field. For weakly driven convection (i.e., low Rayleigh number) the columns described above dominate the flow and have helicity of one sign in the northern and of the opposite sign in the southern hemisphere. The helicity is known to play a crucial role for the dynamo process. The so-called α^2-dynamo mechanism, described by Kageyama and Sato [41] and Olson *et al.* [8], can be thought of as a process where the helicity associated to each convective column produces its own magnetic field. The alignment with the rotation axis and the organized helicity guarantees that the sum of these individual contributions adds up to form the dominant axial dipole field. The dynamo equation describing magnetic field generation can, in principle, produce field of either polarity. This symmetry is broken, however, by the presence of a dominant dipolar background field. Only flows with the opposite helicity in one hemisphere can weaken the prevailing magnetic field and lead to reversals.

In order to better characterize the dynamo process in numerical simulations, Aubert *et al.* [13] have introduced the terms magnetic cyclone and magnetic anticyclone. Both are

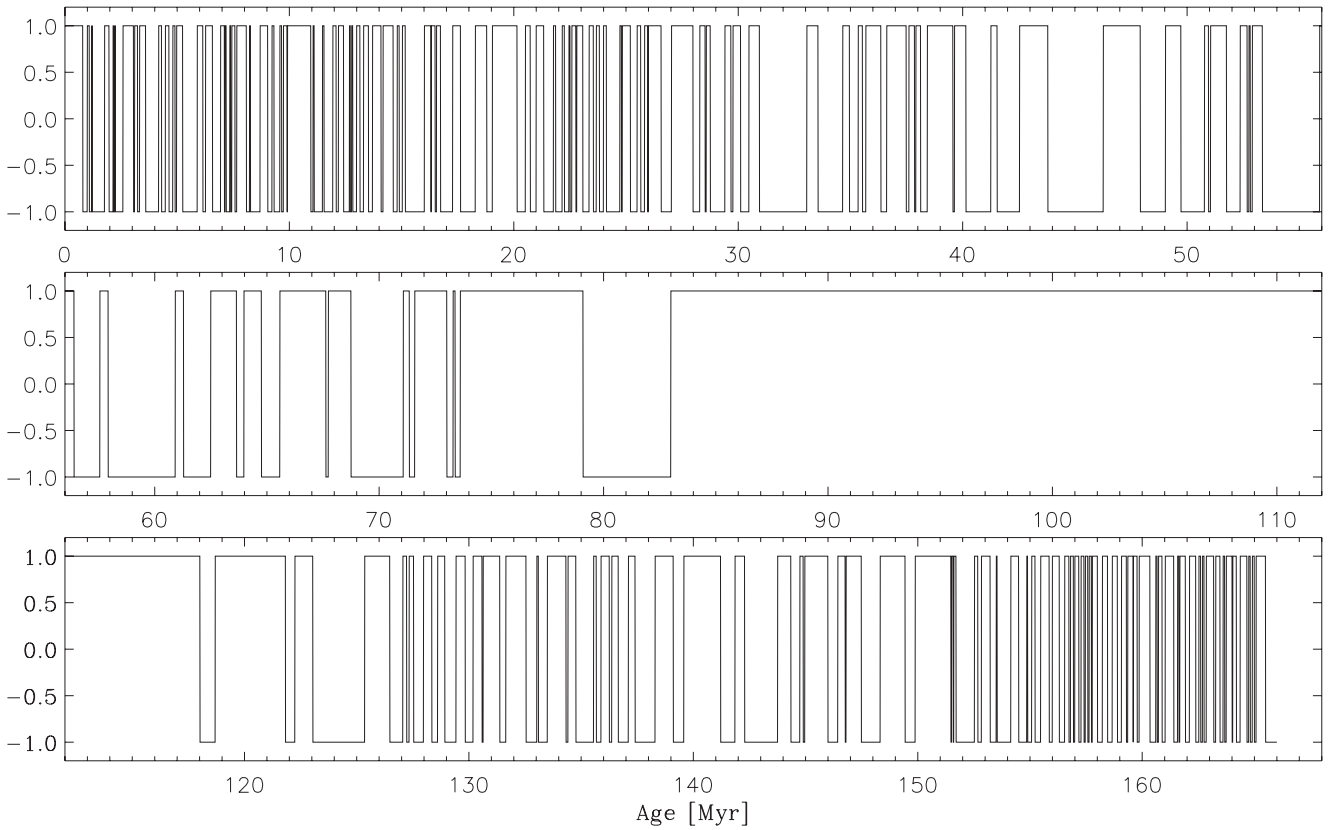

FIG. 10. Geomagnetic reversal record from present to 166 Myr BP. The record comprises 332 reversals. A magnetization of +1 is assigned for chrons with normal polarity and of −1 for chrons with reversed polarity.

directly related to the cyclonic and anticyclonic convective columns. A reversal is initiated when another magnetic structure appears that Aubert *et al.* [13] call "magnetic upwelling." These features are related to radial flow upwellings and can produce inverse magnetic field. While they seem to be a common feature at strong convective driving (i.e., large Rayleigh numbers) they only succeed to trigger a reversal when they are fierce enough to also affect the field produced by the neighboring magnetic cyclones and anticyclones, practically annihilating the prevailing magnetic field. Alternatively, several upwellings can team up to do the job. Once the background field is weak enough, convective columns are free to produce inverse magnetic field, tilting the "local dipole" field over and thereby convincing neighboring columns to follow. The reversal ends once columns producing inverse field dominate. Conceptually, the magnetic upwellings can be understood as columns with the "wrong" helicity.

The potential energy $P(t)$ of Eq. (2) models two effects. Effect one, scaled with γ, is the alignment of the convective columns producing field of either polarity with respect to the rotation axis. Effect two, scaled by λ, models the fact that the polarity that a convective structure produces is strongly influenced by the neighboring field. The second term in the potential energy also models the effect that a tilted spin can convince its neighbors to follow. In the interpretation by Aubert *et al.* [13], that would happen once a magnetic upwelling is strong enough. Without either of these effects, no dominant polarity or stable dipole epoch can emerge.

As the alignment of the spins with the rotation axis is enforced by increasing the absolute value of γ, we expect that the reversal rate goes down as seen in Fig. 8(a). There should be a tradeoff between γ and the random forcing factor ϵ. In MHD simulations, this is probably related to the fact that the Rayleigh number, and thus the convective forcing, has to be increased to compensate a rise in rotation rate Ω (i.e., decreasing Ekman number E) [11].

The diffusive term, scaled with κ in the Langevin Eq. (3), represents the fact that a magnetic field needs time to be generated against magnetic diffusion. Finally, the random forcing term, scaled with ϵ in Eq. (3), encodes the flow fluctuations that seem to trigger reversals in the simulations, for example, the appearance of strong magnetic upwellings. In kinematic dynamo models, this would be described by stochastic α fluctuations [e.g., [24].

If the friction time scale (proportional to κ) becomes shorter than the typical flow time scale (proportional to ϵ), polarity reversals are suppressed consistently with the behavior of the spin model [see Fig. 8(c)]. In the numerical simulations, this is connected to the fact that the Rayleigh number has to be significantly larger than the value at which dynamo action

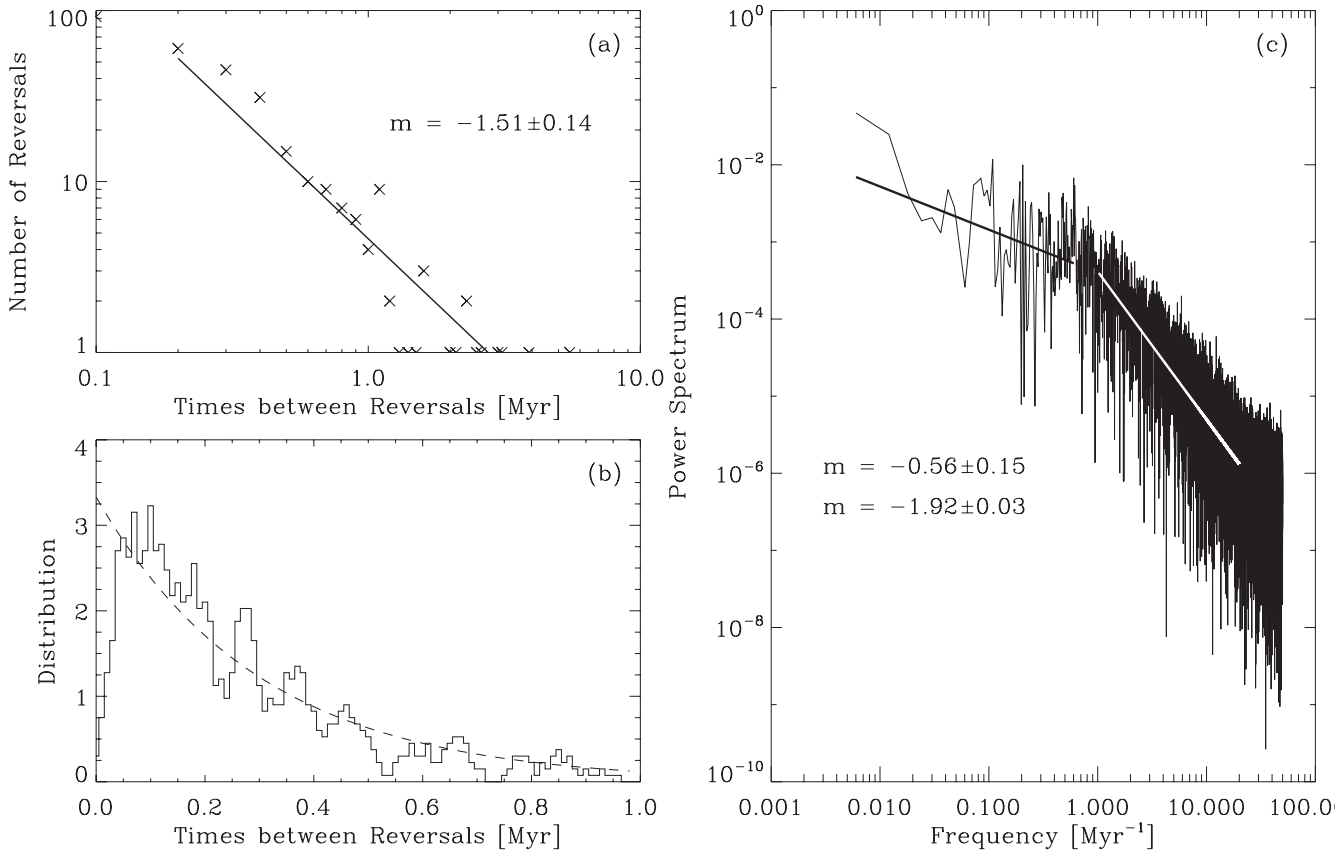

FIG. 11. (a) Log-log plot of the number of reversals as a function of times between reversals of the geomagnetic reversal record shown in Fig. 10. (b) Normalized distribution of the times between reversals for short duration chrons of less than 1 Myr. These make up 298 of the 332 reversals. The bin size here is four times the interval size. The dashed line is the expected probability density function in the case of a Poissonian process with a mean polarity residence time of 300 kyr. (c) Power spectrum of the geomagnetic reversal record.

starts. Increasing ϵ increases the number of reversals as shown in Fig. 8(d). From numerical simulations [16], we know that a stronger convective driving (i.e., larger Rayleigh number) not only leads to more complex behavior in time and space but indeed also to more frequent reversals.

The number of spins is an additional parameter explored here. In the MHD simulations this is not a free parameter, but the number of columns is known to increase with increasing Ω (i.e., with decreasing E). Since the numerics then become increasingly difficult, the effect on the reversal rate has not really been explored so far. Statistically meaningful results only exist for relatively small rotation rates (large E) [20].

In conclusion, though the spin model is only a rough parametrization of the reversal dynamics in a full 3D dynamo simulation, it nevertheless seems to capture the main effects.

VI. COMPARISON WITH GEOMAGNETIC DATA

We use the geomagnetic polarity time scale of Cande and Kent [42,43] and Ogg [44], which covers the past 166 Myr and comprises 332 reversals. Assigning a magnetization of $+1$ for chrons of normal polarity and -1 for chrons of reversed polarity we derive Fig. 10, which is an analog to Fig. 2. Reversals occurred at irregular intervals of 10^5 to 10^7 yr. The mean time between reversals is approximately 300 kyr, whereas reversals are fast events lasting only a few kyr. The reversal frequency has considerably decreased toward and increased away from the Cretaceous superchron, which lasted from 118 to 83 Myr BP [15].

The potential nonstationarity of the geomagnetic reversal record is not present in the domino model of Sec. III but could be easily accounted for by a gradual change of the model parameters with time (Sec. IV). This may present some difficulties for the direct comparison of the statistical analysis. The cumulative distribution of polarity chrons roughly follows a power law with an exponent of -1.5 [Fig. 11(a)]. Polarity intervals of a duration shorter than 1 Myr, which make up the vast majority of all intervals, follow an exponential or Poissonian distribution with a mean of 300 kyr [Fig. 11(b)]. Ryan and Sarson [19] find that the full set of polarity intervals is better fitted by lognormal and loglogistic distributions rather than Poisson and gamma distributions [15]. The power spectrum of the geomagnetic record follows power laws with an exponent of about -0.6 for chrons longer than about 3 Myr and an exponent of about -1.9 for chrons of shorter duration [Fig. 11(c)].

As a measure of the short-term variability of the geomagnetic field at times between reversals, we analyze the virtual axial dipole moment (VADM) of the SINT-2000 data set [Fig. 12(a)] [45]. The power spectrum of these fluctuations with a characteristic power index of -3 is displayed in Fig. 12(b), while the distribution of the VADM is given in Fig. 12(c). For a comparison of the distribution derived from the shorter SINT-800 data set of Guyodo and Valet [46], see Hoyng *et al.* [47].

When comparing the geomagnetic data with the behavior of our reference model illustrated in Figs. 3 and 4, striking similarities become apparent. The fits to the chron durations suggest similar power law exponents of approximately -1.5

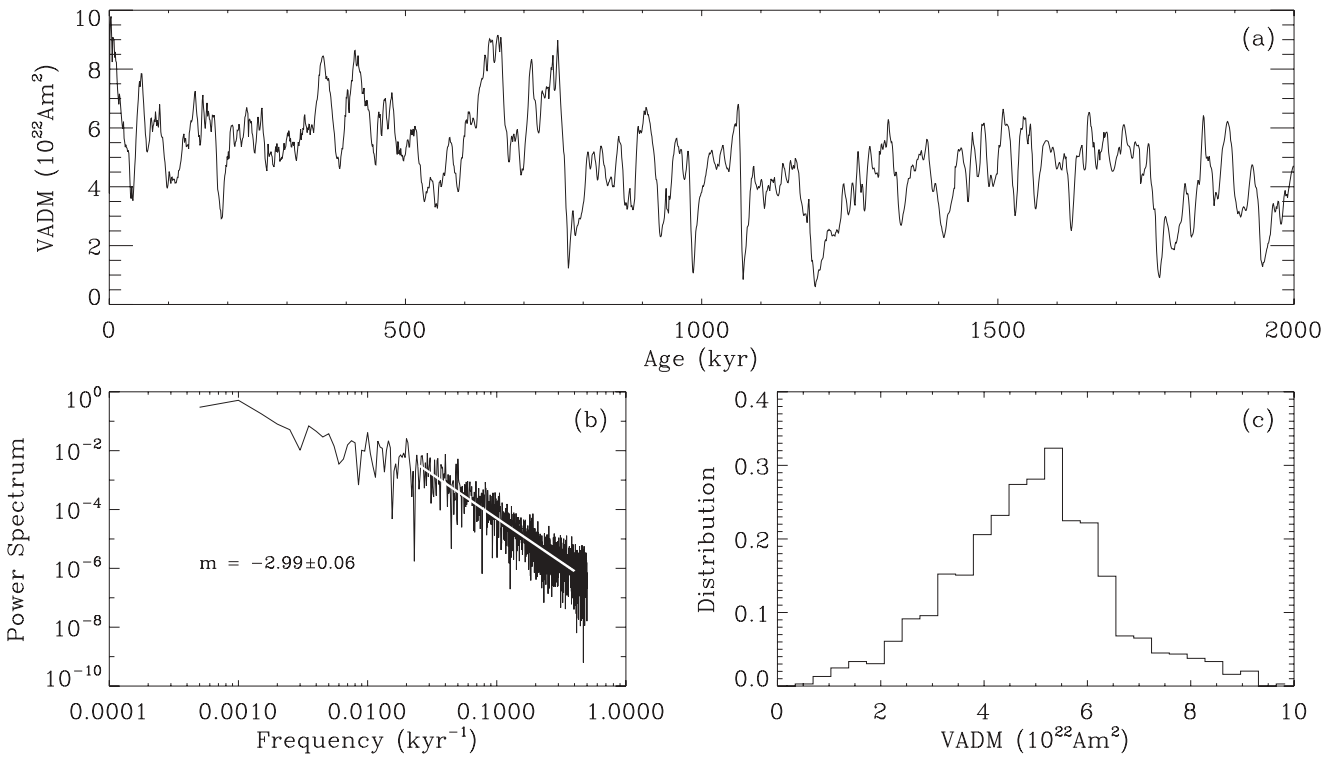

FIG. 12. (a) Variability of the virtual axial dipole moment (VADM) during the past 2 Myr, the SINT-2000 data set. The absolute values of the VADM are given, disregarding the five reversals during this period. (b) Power spectrum of the VADM time series. (c) Distribution of the VADM.

for the paleomagnetic sequence and for our simple model. In the latter, we have disregarded the short chrons, which seem to represent brief statistical ventures into the other polarity because they follow a different behavior. These may be identified with paleomagnetic excursions.

The power spectrum of the geomagnetic reversal record [Fig. 11(c)] only refers to polarity epochs and, therefore, does not contain the high-frequency contributions in our model [Fig. 3(c)]. The low-frequency range can be interpreted as the background variation in the reversal frequency. This leaves us with comparing the midfrequency spectrum with a slope of -1.9 for the paleomagnetic data and -1.7 for our model. The high frequency part of the model can be compared with the SINT data analysis, which yield a slope of -3 compared to -6 in the model. Not surprisingly, this discrepancy suggests that our model does a good job in replicating the statistics of the reversals, but not in the details of the secular variation. A detailed discussion of the power spectrum of reversals as well as intensities is presented in Constable and Johnson [48].

VII. DISCUSSION AND CONCLUSIONS

Our simple domino model of interacting magnetic spins reproduces the qualitative features of geomagnetic polarity reversals remarkably well. The orientation of the aggregate of all spins is most of the time nearly aligned or antialigned and deviates only slightly from the rotational axis. Once in a while, at sporadic times, it starts flipping to ultimately change the orientation by almost 180 degrees or to move back to the original direction. The model thus mimics sporadic reversals of polarity, excursions, and secular variation of the geomagnetic dipole field. The power spectrum derived from the paleomagnetic reversal records as well as the distribution of the virtual axial dipole moment are qualitatively well represented in the model. Furthermore, the statistics of the times between reversals is similar in the model and in the case of the Earth's magnetic field.

Our model provides a convincing statistical representation of the geomagnetic field reversals process. One should be careful, however, when interpreting the model properties in terms of magnetohydrodynamics. Secular variation, which is mainly determined by the details of the convective flow dynamics, is certainly not captured correctly. The view that the convective columns to a certain degree represent building blocks of the full dynamo process seems to be strengthened by our results. A stable polarity can only be established when the majority of these entities cooperate and produce fields of the same polarity. Random forcing counteracts this and may sometimes be violent enough to cause a spin to flip significantly and leave the team. This may cause its neighbors to follow and ultimately lead to a global reversal. The magnetic upwellings identified in full 3D dynamo simulations by Aubert *et al.* [13] could be these events. When these upwellings last long enough or produce enough inverse field, they disrupt the normal dynamo process. The statistics of the complex interplay of many agents seems to be nicely describable by our domino model of a Vaks-Larkin-type set of interacting magnetic spins.

ACKNOWLEDGMENTS

N.M. acknowledges financial support by the Max Planck Institute for Solar System Research. The research of A.F.M. has been partially funded by the Spanish Ministerio de Ciencia e Innovación and Ministerio de Economía y Competitividad, through Projects No. AYA2009-14105-C06-06 and No. AYA2011-29833-C06, including European FEDER funds. This work benefited from A.F.M.'s visit to the Universities of Tokyo and Kyoto supported by a grant from the Japanese Society for the Promotion of Science (JSPS).

[1] J. A. Jacobs, *Reversals of the Earth's Magnetic Field* (Cambridge University Press, Cambridge, 1994).
[2] R. T. Merrill, M. W. McElhinny, and P. L. McFadden, *The Magnetic Field of the Earth: Paleomagnetism, the Core, and the Deep Mantle* (Academic Press, San Diego, 1998).
[3] M. Berhanu, R. Monchaux, S. Fauve, N. Mordant, F. Pétrélis, A. Chiffaudel, F. Daviaud, B. Dubrulle, L. Marié, F. Ravelet, M. Bourgoin, Ph. Odier, J.-F. Pinton, and R. Volk, Eur. Phys. Lett. **77**, 59001 (2007).
[4] G. A. Glatzmaier and P. H. Roberts, Nature (London) **377**, 203 (1995).
[5] H. Amit, R. Leonhardt, and J. Wicht, Space Sci. Rev. **155**, 293 (2010).
[6] P. H. Roberts, in *Treatise on Geophysics*, edited by G. Schubert (Elsevier, Amsterdam, 2007), Vol. 8, p. 67.
[7] F. H. Busse, Geophys. J. Roy. Astron. Soc. **42**, 437 (1975).
[8] P. Olson, U. R. Christensen, and G. A. Glatzmaier, J. Geophys. Res. **104**, 10383 (1999).
[9] U. R. Christensen and J. Wicht, in *Treatise on Geophysics*, edited by G. Schubert (Elsevier, Amsterdam, 2007), Vol. 8, p. 245.
[10] C. Kutzner and U. R. Christensen, Phys. Earth Planet. Inter. **131**, 29 (2002).
[11] U. R. Christensen and J. Aubert, Geophys. J. Int. **116**, 97 (2006).
[12] P. Olson and U. R. Christensen, Earth Planet. Sci. Lett. **250**, 561 (2006).
[13] J. Aubert, J. Aurnou, and J. Wicht, Geophys. J. Int. **172**, 945 (2008).
[14] A. J. Biggin, B. Steinberger, J. Aubert, N. Suttie, R. Holme, T. H. Torsvik, D. G. van der Meer, and D. J. J. van Hinsbergen, Nature Geosci. **5**, 526 (2012).
[15] C. Constable, Phys. Earth Planet. Inter. **118**, 181 (2000).
[16] P. Driscoll and P. Olson, Earth Planet. Sci. Lett. **282**, 24 (2009).
[17] G. A. Glatzmaier, R. S. Coe, L. Hongre, and P. H. Roberts, Nature (London) **401**, 885 (1999).
[18] A. R. T. Jonkers, Phys. Earth Planet. Inter. **135**, 253 (2003).
[19] D. A. Ryan and G. R. Sarson, Geophys. Res. Lett. **34**, L02307 (2007).
[20] J. Wicht, S. Stellmach, and J. Harder, in *Geomagnetic Field Variations*, edited by K.-H. Glaßmeier, H. Soffel, and J. F. W. Negendank (Springer, Berlin, 2009), p. 107.

[21] T. Rikitake, Proc. Cambridge Phil. Soc. **54**, 89 (1958).
[22] M. Shimizu and Y. Honkura, J. Geomag. Geoelectr. **37**, 455 (1985).
[23] H. M. Ito, J. Stat. Phys. **53**, 19 (1988).
[24] P. Hoyng, M. A. J. H. Ossendrijver, and D. Schmitt, Geophys. Astrophys. Fluid Dynamics **94**, 263 (2001).
[25] D. Schmitt, M. A. J. H. Ossendrijver, and P. Hoyng, Phys. Earth Planet. Inter. **125**, 119 (2001).
[26] W. Greiner, L. Neise, and H. Stöcker, *Thermodynamics and Statistical Mechanics* (Springer, New York, 1995).
[27] V. H. A. Dias, J. O. O. Franco, and A. R. R. Papa, Braz. J. Phys. **38**, 12 (2008).
[28] A. Mazaud and C. Laj, Earth Planet. Sci. Lett. **92**, 299 (1989).
[29] M. Seki and K. Ito, J. Geomag. Geoelectr. **45**, 79 (1993).
[30] V. G. Vaks and A. I. Larkin, Sov. Phys. JETP **22**, 678 (1966).
[31] H. E. Stanley, *Introduction to Phase Transitions and Critical Phenomena* (Oxford University Press, Oxford, 1987).
[32] A. C. Hindmarsh [http://www.netlib.org/odepack] (2001).
[33] A. Nakamichi, H. Mouri, D. Schmitt, A. Ferriz-Mas, J. Wicht, and M. Morikawa, Mon. Not. R. Astron. Soc. **423**, 2977 (2012).
[34] C. Bouligand, G. Hulot, A. Khokhlov, and G. A. Glatzmaier, Geophys. J. Int. **161**, 603 (2005).
[35] S. Kida and H. Kitauchi, Progr. Theoret. Phys. Suppl. **130**, 121 (1998).
[36] C. Kutzner and U. R. Christensen, Geophys. J. Int. **157**, 1105 (2004).
[37] G. R. Sarson and C. A. Jones, Phys. Earth Planet. Inter. **111**, 3 (1999).
[38] F. Takahashi, M. Matsushima, and Y. Honkura, Science **309**, 459 (2005).
[39] J. Wicht, Geophys. J. Int. **162**, 371 (2005).
[40] J. Wicht and P. Olson, Geochem. Geophys. Geosyst. **5**, Q03H10 (2004).
[41] A. Kageyama and T. Sato, Phys. Rev. E **55**, 4617 (1997).
[42] S. C. Cande and D. V. Kent, J. Geophys. Res. **97**, 13917 (1992).
[43] S. C. Cande and D. V. Kent, J. Geophys. Res. **100**, 6093 (1995).
[44] J. G. Ogg, in *Global Earth Physics—A Handbook of Physical Constants*, edited by T. J. Ahrens (AGU, Washington, 1995), p. 240.
[45] J.-P. Valet, L. Meynadier, and Y. Guyodo, Nature (London) **435**, 802 (2005).
[46] Y. Guyodo and J.-P. Valet, Nature (London) **399**, 249 (1999).
[47] P. Hoyng, D. Schmitt, and M. A. J. H. Ossendrijver, Phys. Earth Planet. Inter. **130**, 143 (2002).
[48] C. Constable and C. Johnson, Phys. Earth Planet. Int. **153**, 61 (2005).